ISSN (Online) 2456-1290

International Journal of Engineering Research in Mechanical and Civil Engineering (IJERMCE)
Vol 3, Issue 2, February 2018

PERFORMANCE CHARACTERISTICS OF MULTI CYLINDER PRE HEATED AIR WITH TURBOCHARGED ETHANOL DIRECT INJECTION ON CI ENGINE WITH EGR

[1] M. Velliangiri, [2] M. Karthikeyan
[1][2] Assistant Professors Department of Mechanical Engineering
Coimbatore Institute of Technology- Tamilnadu- INDIA

Abstract:-- **This article focused on the simulation, experimental study of performance parameters, exhaust gas recirculation, heat release rate for multicylinder preheated turbocharge direct injection ultra-high compression ignition engine. Simulation results, methodology, combustion models, sub-models were used to find optimised performance parameters for better combustion. Optimum piston bowl parameters were identified by conducting a test with constant compression ratio (28.54:1) and constant speed mode (1500 rpm) by varying Exhaust Gas Recirculation (EGR) ratio between 0 to 15%, and emission characteristics were found. Optimised EGR ratio among the variations and predicted suitable ignition timing and duration for ethanol HCI engine were selected from simulation results. Variation of In-cylinder pressure, heat release rate with Crank Angle and Specific Fuel Consumption, Ignition Delay, along with NOx and Particulate Matter emission results were obtained from the simulation and experimental results. Simulation results were exploited to choose better combustion with less fuel consumption. A partial preheating of exhaust gas is performed to boost the intake air temperature to 65 deg C. The experiments were done with a randomly selected set of 7 injection holes and their expected ignition delay. Ignition delay was reduced, and the NOx reduction hit about 76 percent, while the EGR rise provided a 0.6-0.9 percent increase while burning higher percentages of fuel.**

Index Terms:- preheated turbocharged, Heat Release Rate, EGR optimisation, Ignition delay, Ethanol High compression Ignition, Swirl Ratio

1. INTRODUCTION

Current internal combustion (IC) engine research is very tough due to substantial exhaust gas emission restrictions and Green House Gas (GHG) emissions like CO2 emissions, NOx and particulate matter (PM). The instability of the fossil fuel reserves emphasises the necessity to continue developing high combustion efficiency low fuel consumption engines that operate with renewable energy sources like bioethanol fuel engine. [1]. Apart from the GHG emission (CO2), the emissions legislation restricts the NOx and particle matter (PM) emissions to ultra-low values and continues to almost zero emissions[2]. Multi-cylinder CI engine plays a significant role in the transporting and power generation sector and necessary to control the combustion process, heat release rate, emission characteristics and required to meet the emission norms[3]. Hence, it required optimising combustion and predicting the suitable EGR ratio for diesel and ethanol fuel engine applications for controlling the NOx and PM [4]. Also, to select suitable EGR ratio and piston bowl design modifications, they must meet better combustion and emission norms and acceptable engine performance parameters[5][6]. Hence, this research article focused on developing the new biofuel engine, achieving low emission and soot-free combustion. Ethanol direct injection compression ignition with preheated turbocharged is a big task for initiate the combustion and controlling the temperature of intake air and select the best EGR ratio among the variation of EGR, and required better swirl ratio piston bowl chamber[7]. In addition to this, preheated turbocharged technology was required to increase the intake air temperature for increasing the in-cylinder temperature and find the performance parameters like Specific Fuel Consumption (SFC), Nitrogen Oxides (NOx), Particulate Matter (PM) and Ignition Delay (ID) of the ethanol-fuelled engine[8][9]. Multicylinder engine simulation results obtained from Diesel RK thermodynamic simulations with variable EGR ratio and different swirl ratios pistons[10][11]. Simulation and experimental results were used and plotted concerning various performance and compared for three different EGR ratio and selection suitable chamber for better combustion and low emission[12][13]. Ethanol fuel required ignition improver due to low cetane NO, and high

IFERP
connecting engineers... developing research

ISSN (Online) 2456-1290

International Journal of Engineering Research in Mechanical and Civil Engineering (IJERMCE)
Vol 3, Issue 2, February 2018

SelfIgnition temperature compare to diesel fuel[14]. Hence, the engine compression ratio is increased from 16 to 28.54:1 and preheated turbocharged technology was used to increase the intake air temperature[14].

.

2. Methodology and Experimental setup

Multicylinder preheated turbocharge CI engine combustion simulation methodology has one of the significant phases of the in-cylinder model and predicts the engine parameters[15]. It deals with to create three different EGR ratio and constant swirl ratio piston bowls and a selection of suitable EGR bowl chambers[16]. Based on the methodology, the EGR ratio, bowl chambers parameters created with constant swirl ratio and same compression ratio 16.5:1 for multi-cylinder pre-cooled turbocharged diesel DI engine.

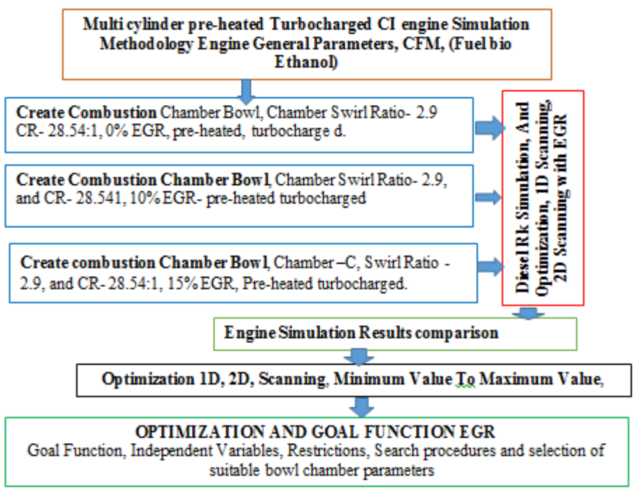

Figure 2.1 Diesel RK simulation methodology for Multi-cylinder ethanol engine

engine[17]. The second is to select suitable multi-hole injectors, which varies from 3 to 7 holes and three different piston bowls with different swirl ratios with the same compression ratio 28.54:1 for multicylinder preheated turbocharged ethanol HCI engine.

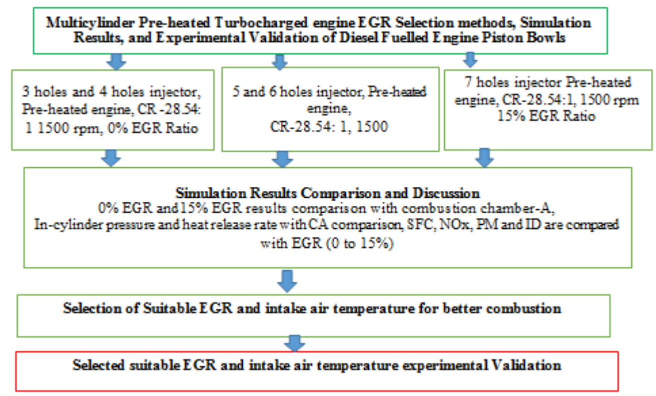

Figure 2.2 Multicylinder Preheated turbocharged engine simulation methodology

Hence, this is a great challenge to create and select a better combustion chamber and select a suitable EGR ratio for low NOx emission and high efficiency[18]. The simulation split into two phases, the first phase was focused on performing and predicting suitable injector holes due to increasing the volume of fuel injection and EGR for better combustion for ethanol engine and the second phase was concentrated to select suitable combustion chamber bowl for ethanol HCI engine as shown in Figure 2.1, 2.2., and 2.3.[19][20] Diesel RK combustion simulation is well supported to find the significance of piston bowl parameters, namely compression ratio (CR) swirl ratio (SR), Exhaust Gas recirculation (EGR), and injection timing (IT), injection pressure (INJP). Cycle fuel mass (CFM) and find optimum combustion and fabrication piston bowl points to achieve better combustion and experiment results and discussed[11]. Injector selection methods are a significant step for ethanol engines due to a 1.6 times lower calorific value than diesel fuel. Hence required to select suitable injectors for injecting required injection duration.

Diesel RK software is well supported to design the Injector like the number of holes, angle of injection, and the results of visualisation of fuel spray in different zones. It can also save as windows graphics files, namely AVI or animated GIF files[21]. Visualisation data was supported to find a spray pattern and plot a picture, as in 3D and shown in Figure 3.2[21]. The evolution of fuel sprays and their Near Wall Flow (NWF) in a combustion chamber and the swirl's effect are predicted and presented hereunder. The deformation of sprays by swirl can predict NWF depending on the angle of sprays and wall impingement[22]. Evolution of NWF under the effect of a swirl and NWF interaction among themselves and Fuel allocation study for the distinct zones. The injection rate and heat release curves can also be studied for spray visualisation in Diesel RK simulation[19].

International Journal of Engineering Research in Mechanical and Civil Engineering (IJERMCE)
Vol 3, Issue 2, February 2018

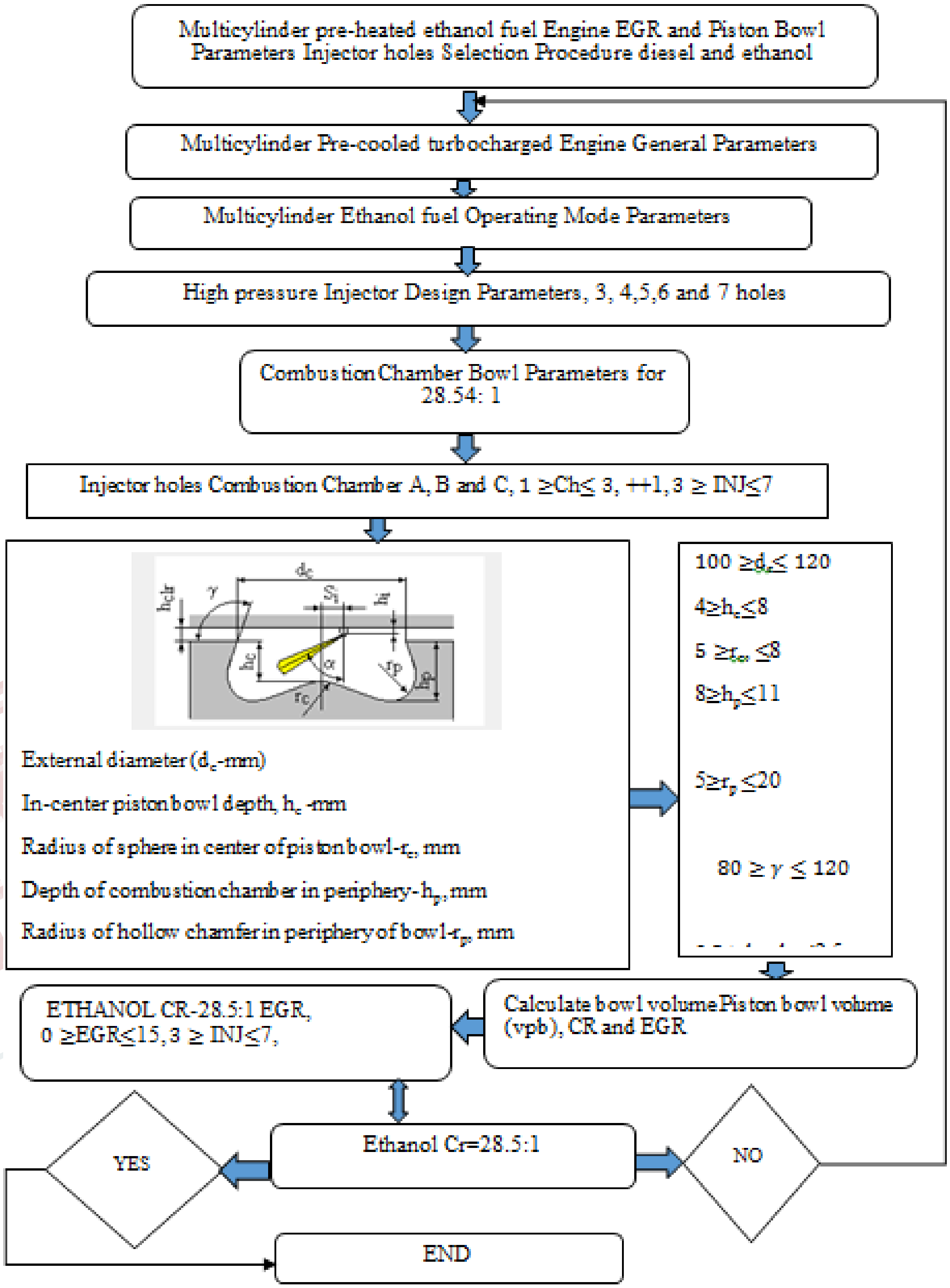

Figure 2.3 Multicylinder preheated ethanol fuel Engine Piston Bowl Parameters, injector holes Selection Procedure

IFERP connecting engineers... developing research

ISSN (Online) 2456-1290

International Journal of Engineering Research in Mechanical and Civil Engineering (IJERMCE)

Vol 3, Issue 2, February 2018

Multicylinder pre-heated turbocharged high compression ignition engine required suitable combustion chamber bowl parameters for better combustion and selection of suitable among the one; this is a practical approach. Hence, a methodology was developed and used to create three different combustion chambers A, B and C, with different swirl ratio, both diesel and ethanol, shown in Figure 2.3.[23] The three different combustion bowl parameter is necessary to predict better combustions.

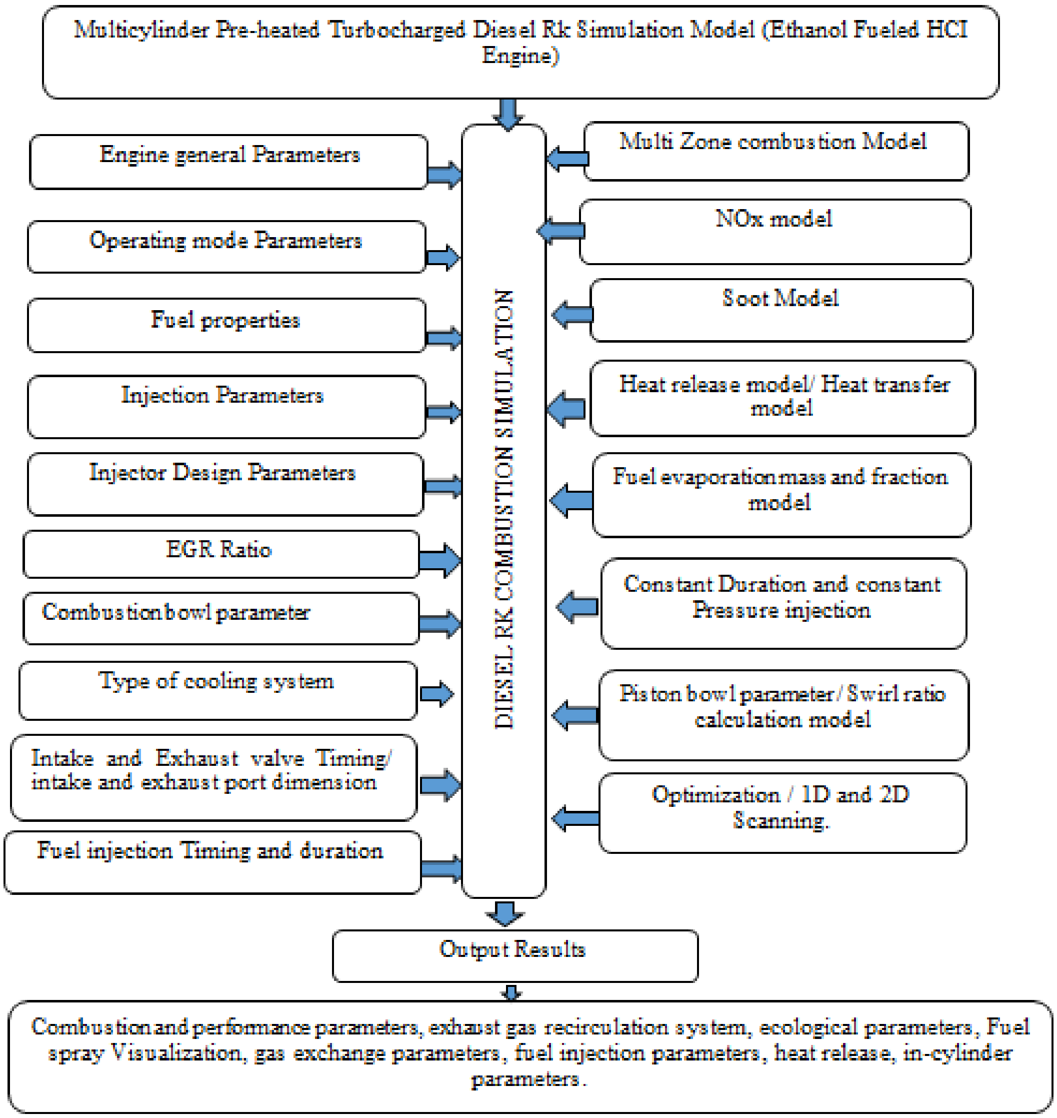

Figure 2.4 Multicylinder Preheated Turbocharged Diesel Rk Simulation Model (Ethanol Fueled HCI Engine)

Swirl ratio is one of the very significant parameters of CI engine combustion. The swirl ratio is well defined by the new charge movement (e.g. air) around the cylinder axis in the IC engine's cylinder [5]. Also, the ratio is essential for mixture preparation to initiate better combustion for ethanol engine to specific swirl. CI engine combustion bowl parameters like bowl external diameter, dc, [mm] 100 to 120, and geometry parameters details were shown in table 1. combustion chamber bowl parameters selection methodology is an efficient approach and challenging task and used to create three different combustion chambers a, b and c with different swirl ratio both diesel and ethanol. It influenced the chamber's control surface to increase thermal efficiency due to the heat transfer rate and heat release rate.[24]

IFERP
connecting engineers... developing research

ISSN (Online) 2456-1290

International Journal of Engineering Research in Mechanical and Civil Engineering (IJERMCE)
Vol 3, Issue 2, February 2018

2.1 In-cylinder pressure Vs Crank angle simulation model

$$R_{bs} = \frac{B}{L}$$

$$x(\theta) = (\lambda + R) - \left(R\cos(\theta) + \left(\left(\lambda^2 - \sin^2(\theta)\right)\right)^{\frac{1}{2}}\right)$$

$$V(\theta) = V_c + \frac{\pi D^2}{4} x(\theta)$$

$$A_h(\theta) = \frac{\pi D^2}{4} + \frac{\pi D S}{2}\left(R + 1 - \cos(\theta) + \left(R^2 - \sin^2(\theta)\right)^{1/2}\right)$$

$$S_p = \frac{ds}{dt} \quad , \quad S_p = \frac{\pi}{2} \sin\theta \left[1 + \frac{\cos\theta}{(R^2 - \sin^2\theta)^{\frac{1}{2}}}\right]$$

$$\frac{dQ_{gr}}{d\theta} = \frac{1}{1-\gamma}\left[\gamma p \frac{dv}{d\theta} + V\frac{dp}{d\theta} + (u - C_v T)\frac{dm_c}{d\theta}\right] - \sum h_i \frac{dm_i}{d\theta} + \frac{dQ_{ht}}{d\theta}$$

$$\frac{dp}{d\theta} = \frac{\gamma - 1}{V}\left(\frac{dQ_{in}}{d\theta} - \frac{dQ_{loss}}{d\theta}\right) - \gamma \frac{p}{v}\frac{dV}{d\theta} + \frac{p}{\gamma - 1}\frac{dk}{d\theta}$$

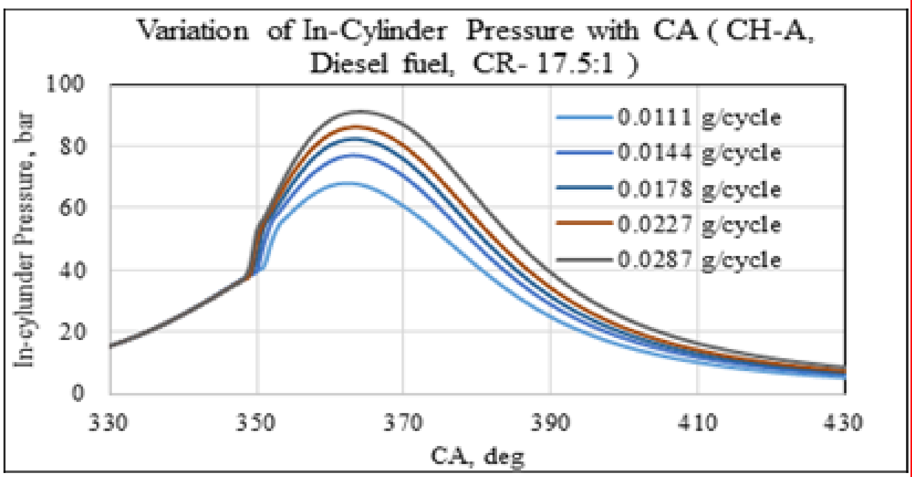

Figure 2.4 In-cylinder pressure Vs Crank angle simulation model

2.2 Simulation of NOx Formation with Crank Angle Simulation Model

IFERP connecting engineers... developing research
ISSN (Online) 2456-1290
International Journal of Engineering Research in Mechanical and Civil Engineering (IJERMCE)
Vol 3, Issue 2, February 2018

$$R_{bs} = \frac{B}{L} \quad ,x(\theta) = (\lambda + R) - \left(R\cos(\theta) + \left(\left(\lambda^2 - \sin^2(\theta)\right)\right)^{\frac{1}{2}}\right)$$

$$V(\theta) = V_c + \frac{\pi D^2}{4} x(\theta), S_p = \frac{ds}{dt}\ ,\ S_p = \frac{\pi}{2}\sin\theta\left[1 + \frac{\cos\theta}{(R^2 - \sin^2\theta)^{\frac{1}{2}}}\right]\ ,$$

$$AF_C = AF_{ini} + \frac{1 - AF_{ini}}{\varphi_z}\varphi$$

$$\frac{dQ_{gr}}{d\theta} = \frac{1}{1-\gamma}\left[\gamma p \frac{dv}{d\theta} + V\frac{dp}{d\theta} + (u - C_v T)\frac{dm_c}{d\theta}\right] - \sum h_i \frac{dm_i}{d\theta} + \frac{dQ_{ht}}{d\theta}$$

$$\frac{dp}{d\theta} = \frac{k-1}{V}\left(\frac{dQ_{in}}{d\theta} - \frac{dQ_{loss}}{d\theta}\right) - k\frac{p}{v}\frac{dV}{d\theta} + \frac{p}{k-1}\frac{dk}{d\theta}$$

$$\frac{d[N]}{dt} = kf_2[N_2][O] - kf_2[N_2][O_2] - kf_3[N][OH] \approx 0\ [N] = \frac{kf_1\ [N_2][O]}{kf_2[O_2] + kf_3\ [OH]}$$

$$\frac{d[NO]}{dt} = kf_1[N_2][O] + kf_2[N][O_2] \cong 2kf_1[N_2][O]$$

$$\frac{d[NO]}{dt} \cong kf_1[N_2][O] \cong 1.476.10^{15}[N_2][O_2]^{\frac{1}{2}} \exp\left(-\frac{67{,}520}{T}\right)\left(\frac{mole}{cc} - s\right)$$

$$\frac{dr_{NO}}{d\varphi} = \frac{p.2.333.10^7.e^{-38020/T_{cz}}.r_{N_2eq}.r_{Oeq}.\left[1 - \left(\frac{r_{NO}}{r_{NOeq}}\right)^2\right]}{RT_{cz}\left[1 + \frac{2346}{T_{cz}}.e^{\frac{3365}{T_{cz}}}.\frac{r_{NO}}{r_{O_2eq}}\right]}\frac{1}{\omega}$$

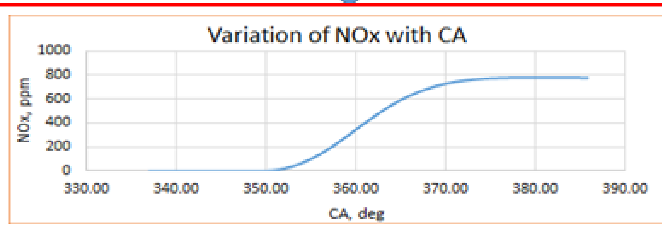

Figure 2.4 simulation of NOx formation with Crank Angle Simulation Model

2.3 Simulation of Heat Release Rate with Crank Angle Simulation Model

IFERP connecting engineers... developing research
ISSN (Online) 2456-1290
International Journal of Engineering Research in Mechanical and Civil Engineering (IJERMCE)
Vol 3, Issue 2, February 2018

$$\delta Q_{in} = de + \delta w + \delta Q_{loss} - \sum h_i m_i$$

$$\Downarrow$$

$$\delta Q_{in} = m c_v dT + p dv + \delta Q_{loss}$$

$$\Downarrow$$

$$\delta Q_{in} = \left(\frac{\lambda}{\lambda - 1}\right) p dv + \frac{1}{\lambda - 1} v dp + \delta Q_{loss}$$

$$\Downarrow$$

$$\delta Q_{in} - \delta Q_{loss} = \left(\frac{\lambda}{\lambda - 1}\right) p dv + \frac{1}{\lambda - 1} v dp$$

$$\Downarrow$$

$$\frac{dQ_{net}}{d\theta} = \left(\frac{\lambda}{\lambda - 1}\right) \frac{p dv}{d\theta} + \frac{1}{\lambda - 1} \frac{v dp}{d\theta}$$

$$\Downarrow$$

$$x(\theta) = (\lambda + R) - \left(R\cos(\theta) + \left(\left(\lambda^2 - \sin^2(\theta)\right)\right)^{\frac{1}{2}}\right)$$

$$\Downarrow$$

$$V(\theta) = V_c + \frac{\pi D^2}{4} x(\theta)$$

$$\Downarrow$$

$$\frac{dV}{d\theta} = \frac{V_d}{2} \sin\theta \left[1 + \frac{\cos\theta}{\sqrt{R^2 - \sin^2\theta}}\right]$$

$$\Downarrow$$

$$\frac{dp}{d\theta} = \frac{\gamma - 1}{V}\left(\frac{dQ_{in}}{d\theta} - \frac{dQ_{loss}}{d\theta}\right) - \gamma \frac{p}{v}\frac{dV}{d\theta} + \frac{p}{\gamma - 1}\frac{dk}{d\theta}$$

$$\Downarrow$$

$$\frac{dQ_{net}}{d\theta} = \frac{1}{1 - \gamma}\left[\gamma p \frac{dv}{d\theta} + V \frac{dp}{d\theta} + (u - C_v T)\frac{dm_c}{d\theta}\right] - \sum h_i \frac{dm_i}{d\theta} + \frac{dQ_{ht}}{d\theta}$$

Figure 2.4 simulation of Heat Release Rate with Crank Angle Simulation Model

The preheated turbocharged multicylinder engine was used to conduct the experiment and diesel RK simulation[25]. The preheated air is used to increase the in-cylinder temperature and well supported to initiate the ethanol direct injection compression ignition. Ethanol fuel has a high latent heat of evaporation (76 to 820 kJ/kg) and high auto-ignition temperature (480 0C); hence high-temperature air is required to initiate the combustion[26]. However, the two ways to increase the in-cylinder temperature one is to increase the compression ratio, and another one is preheated air[27].

Hence, these two methods used to multicylinder turbocharged high compression ratio (28.54:1) engine were used to experiment. The peak values in all zones are obtained from the model. The heat release rate with CA gave valuable information on evaporation and premixed combustion and used to predict the combustion zone and reduce the premixed zone peak value for control of the NOx and PM emissions

IFERP connecting engineers... developing research

ISSN (Online) 2456-1290

International Journal of Engineering Research in Mechanical and Civil Engineering (IJERMCE)

Vol 3, Issue 2, February 2018

formation with CA. The in-cylinder pressure and temperature were changed inside the cylinder due to piston travel and heat transfer to the walls.

2.4 Fuel Evaporation Model

$$\left(\rho \frac{4}{3}\pi \frac{d}{dt}\left(\frac{D^3}{2^3}\right)h_{fg}\right) = -\pi D k \frac{T_a - T_b}{C_1}, \qquad \beta_0 = \frac{(4K(T_a - T_b)}{\rho_l h_{fg}}$$

$$2C_1\beta_0 = \frac{(8K(T_a - T_b)}{\rho_l h_{fg}}$$

$$\beta = \frac{1.6 R_{eD}^{\frac{1}{2}} K p_r^{\frac{1}{3}})(T_a - T_b)}{\rho_l h_{fg}}$$

$$\frac{dD^2}{dt} = -2C_1\beta_0 - \beta$$

$$D_t^2 - D_0^2 = -2C_1\beta_0 t - \beta t$$

$$D_t^2 = D_0^2 - 2C_1\beta_0 t - \beta t$$

$$t_{life} = \frac{D_0^2}{2C_1\beta_0 t + \beta t}$$

Figure 2.5-Fuel Evaporation Model

Blow-by gas and work transfer depend on the combustion chamber shape and compression ratio. Therefore, to examine the combustion process, it is necessary to relate each of the above to the pressure rise rate and separate the effect of combustion from the other effects of heat release with CA. It dealt with a fuel evaporation model and fuel injection model to predict droplet size and sprays' evolution. The droplet evaporation rates for CA and ET were predicted using the fuel evaporation model in Figure 2.5. Combustion zones of the fuel injector exist in the fuel spray. The model focuses on finding the best working configuration for high-velocity droplet and dense axial flow core. As the jet of fuel penetrates through the wall, it evaporates the fuel droplet and diminishes its lifetime significantly.

Schematic Diagram of The Experimental Setup

ISSN (Online) 2456-1290

International Journal of Engineering Research in Mechanical and Civil Engineering (IJERMCE)

Vol 3, Issue 2, February 2018

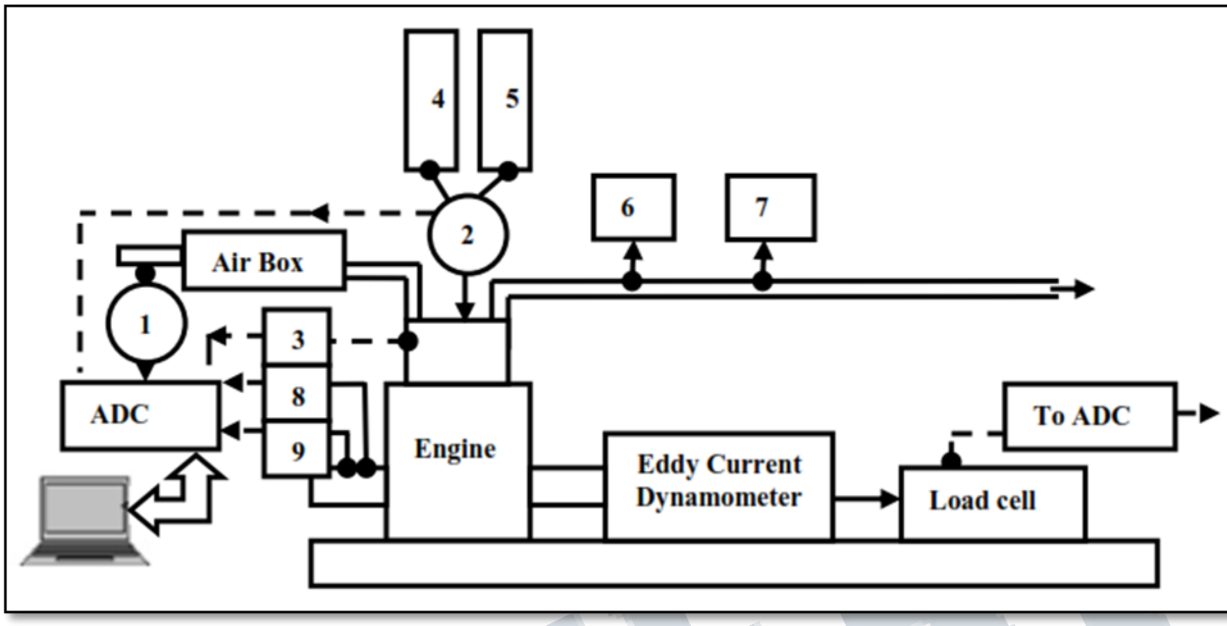

Figure2.6 Schematic diagram of the experimental setup

Airflow sensor, 2. Fuel flow sensor, 3. A pressure sensor, 4. Diesel tank, 5.Ethanol tank, 6. Five gas analysers, 7. Smoke Meter, 8. RPM Indicator, 9. Crank Angle encoder.

Table.1 Specification of the experimental test rig

Make & Model	6 cylinder Kirloskar diesel oil Engine,
Research Engine Type	Four strokes / Water-cooled / CI engine.
Number of cylinder/ Bore/Stroke	One / 150mm /180 mm.
Compression Ratio Diesel/ Ethanol fuel	Diesel 17.5:1/ Ethanol 28.54:1
In-cylinder pressure limit	0 to 240 bar
Engine Direction of rotation/ Speed	Clockwise/ 1500rpm to 1600rpm
Fuel injection timing Diesel fuel engine	23^0BTDC (Adjustable)
Inlet / Exhaust Valve clearance	0.18 mm /0.20mm
Type /Engine oil Lubricating system	Gear type/ Force feed system
Oil Sump capacity /Lubricating oil pump delivery	5.70 liters/6.50 lit/min

The engine with measurement components, namely fuel injection pump, eddy current dynamometer, device for changing fuel, EGR system, Data Acquisition system, Smoke meter, Exhaust gas analyser, and Pressure transducer shown in Figure 2.6. The specifications of the preheated turbocharged engine are given in Table 1. NOx emission was drastically decreased when compared to Engine Power and BMEP. The research work involves both experimental and theoretical investigations. The engine experiments were carried out using a single-cylinder four-stroke CI engine with an eddy current dynamometer. Various experiments conducted served as the validation for the simulation studies carried out in this research. The setup is shown in Figure 2.5 and experimental arrangement, wherein the Exhaust Gas Recirculation and various measurement systems integrated with the core system viz., the Variable Compression Ratio Engine. The measurement systems included the eddy current dynamometer, crank angle encoder and in-cylinder pressure sensors, and fuel and airflow measurement devices. Specifications of National Instruments (NI) Data Acquisition (NI-DAQ) systems were used to gather the engine's performance parameters. Experimental validation of Chamber A and variation of in-cylinder pressure, SFC, BTE and NOx, and without EGR are discussed in this section.

4. Results and Discussion

Diesel RK Simulation Tool and methodology were used to find suitable bowl parameters and created suitable swirl ratio piston bowls for the ethanol engine. Optimisation methodology used to find an optimum point of CR, SR, EGR ratio, injection pressure, and injection timing.

ISSN (Online) 2456-1290

International Journal of Engineering Research in Mechanical and Civil Engineering (IJERMCE)
Vol 3, Issue 2, February 2018

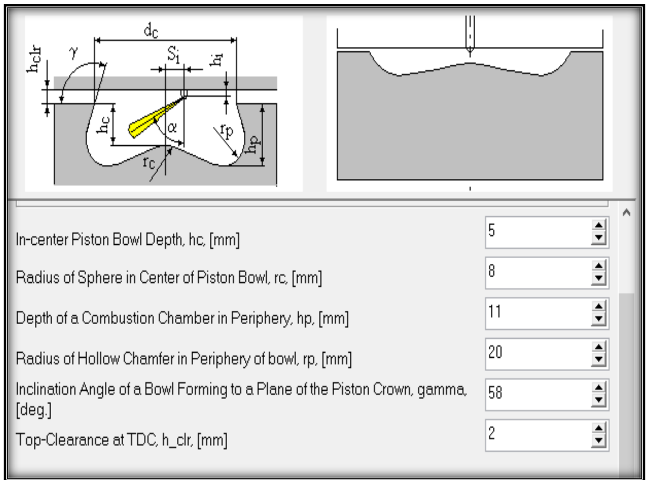

Figure: 3.1 Combustion bowl Chamber

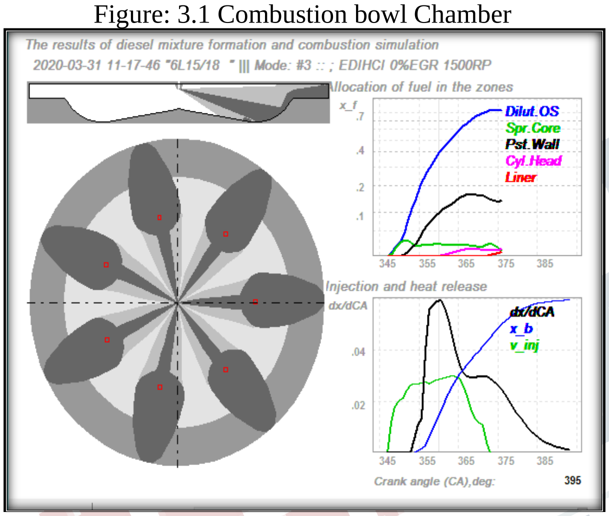

Figure 3.2 Fuel spray visualisation seven holes injection

Diesel Rk simulation tool is used to create a combustion chamber and shown in Figure 3.1, and Fuel spray visualisation was one of the unique features of Diesel RK, as shown in Figure 3.2. This software allows studying the animation picture format of the visualisation and modelling, the fuel spray's interaction with combustion chamber walls, air swirl, and neighbouring sprays. Results of visualisation can be saved as Windows graphics files, AVI or animated GIF files. Visualisation data as possible as a plot a picture, as in 3D and shown in Figure 3.2. The evolution of fuel sprays and their Near Wall Flow (NWF) in a combustion chamber and the swirl effect are discussed and presented hereunder. 1) The deformation of sprays by swirl was predicted. 2) Formation of NWF depending on the angle of sprays and wall impingement. 3) Evolution of NWF under the effect of a swirl and NWF interaction among themselves. 4) Fuel allocation in distinct zones. 5) The curves of injection rate and heat release. In-cylinder heat release rate data can provide information about the combustion phase and percentage of heat release concerning the crank angle. Direct measurements of heat release rates in an IC engine are difficult. However, the heat release rate can be deduced from time histories of in-cylinder pressure with Crank Angle (CA). Diesel RK model and some parameters are presented in the following section

Diesel RK Simulation Tool and methodology were used to find suitable bowl parameters and created suitable swirl ratio piston bowls for the ethanol engine. Optimisation methodology used to find an optimum point of CR, SR, EGR ratio, injection pressure, and injection timing. Both diesel and ethanol simulation results, comparison graphs and suitable parameter selection methods, simulation and experimental results were compared and shown in Figure 4.1 to 4.6.

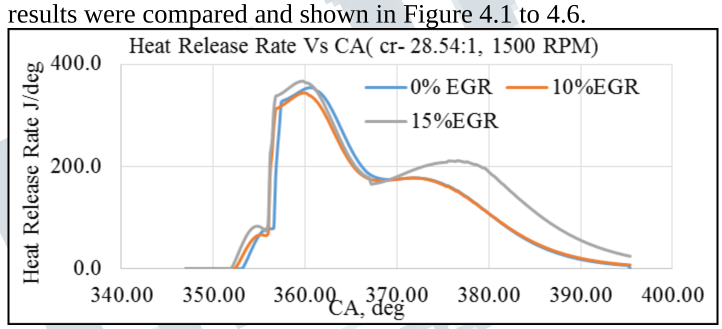

Figure 4.1 Heat Release rate Vs Figure CA

It can be shown that variation of heat release rate(HRR) (J/CA) when increasing the EGR ratio heat release rate curve move 2to 3 deg towards before top dead centre (BTDC). The premixed combustion zone evaporation rate increased, and diffused zone HRR was reached upto201 J/deg and lower than the premixed zone. In the premixed zone peak value of HRR was 343 to 353 J/deg. Based on this, EGR is well supported for combustion and reduced combustion temperature.

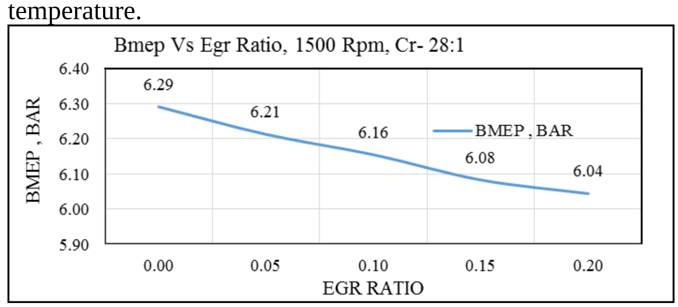

Figure 4.2 Variation BMEP concerning EGR ratio, 1500 rpm, bmep 6.29 bar

The variation of BMEP concerning EGR is shown in Figure 4.2. BMEP varied from 6.29 to 6.04 bar when increasing the EGR ratio from 0 to 15%. The BMEP decreased by 3.97% when compared to 0% EGR. It is concluded that SFC was slightly 0.9 % increased when compared to 0% EGR. But

ISSN (Online) 2456-1290

International Journal of Engineering Research in Mechanical and Civil Engineering (IJERMCE)
Vol 3, Issue 2, February 2018

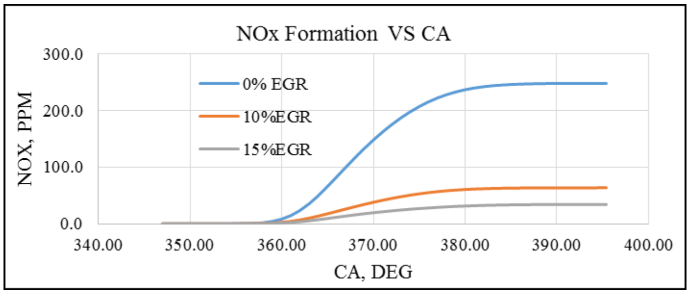

Figure 4.3 Formation of NOx concerning EGR ratio, 1500 rpm, bmep 6.29 bar

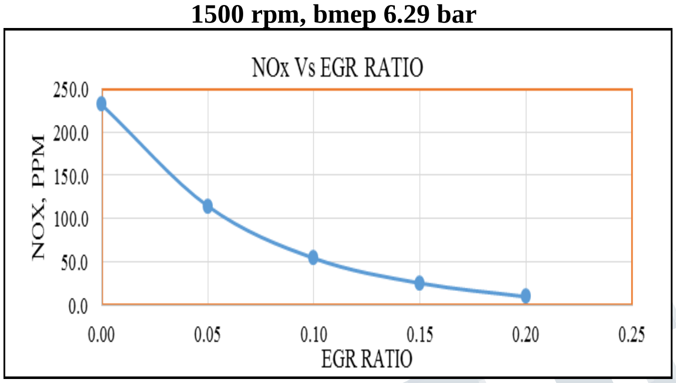

Figure 4.4 Variation NOx concerning EGR ratio, 1500 rpm, bmep 6.29 bar

Combustion performance increased, and NOx emission was decreased and shown in the following graphs. It can be shown that variation NOx concerning EGR ratio and shown in Figure 4.4, when to increase the EGR ratio, the variation of NOx concerning EGR is decreased shown in Figure 4.4. NOx was varied from 232 to 10 ppm when increasing the EGR ratio from 0 to 15%.

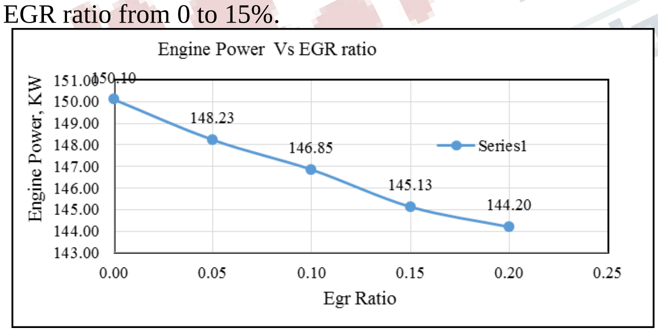

Figure 4.5 Variation Engine Power concerning EGR ratio, 1500 rpm, bmep 6.29 bar

It can be shown that variation Engine Power concerning EGR ratio and In-cylinder pressure

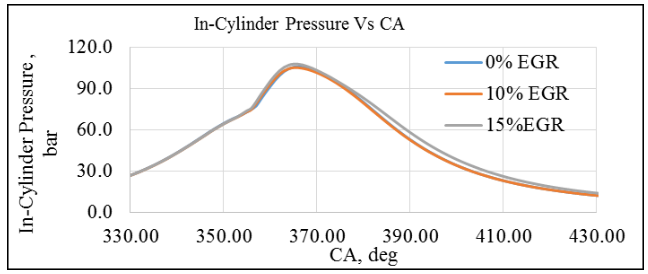

Figure 4.5 Variation Engine Power concerning EGR ratio, 1500 rpm, bmep 6.29 ba

It can be shown that variation Engine Power concerning EGR ratio and In-cylinder pressure concerning CA shown in Figure 4.5 and 4.6 when to increase the EGR ratio the variation of engine Power decreased concerning EGR but in-cylinder is not drastically changed when compared to others shown in Figure 4.5 and 4.6. Engine Power was varied from 150 to 144 kW when increasing the EGR ratio from 0 to 15%. Engine Power (IP) decreased by 4% when compared to 0% EGR. It is concluded that SFC was slightly 0.9 % increased when compared to 0% EGR. But combustion performance

4.2 Experimental results comparison of In-Cylinder Pressure Vs Crank Angle (CA) comparison

Figure 4.7 Pressure Vs CA Comparison of Diesel and Ethanol fuel, 1500 rpm, 0.222 g/Cycle, 0% EGR

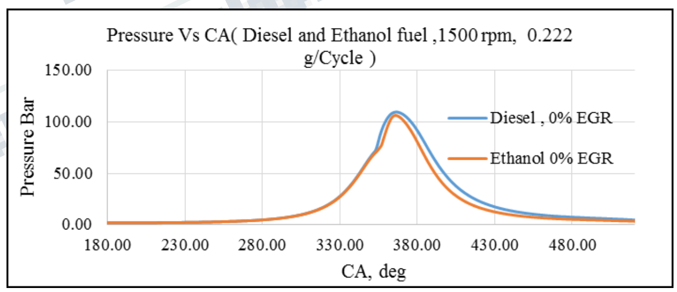

Figure 4.8 Pressure Vs CA Comparison of Diesel and Ethanol fuel,1500 rpm, 0.222 g/Cycle,10% EGR

It can be shown that variation In-Cylinder Pressure with respect to CA and shown in Figure 4.7 to 4.9, In-cylinder Pressure with CA diagram shows that when increasing the EGR ratio (10%) the variation of peak pressure is not drastically changed concerning EGR and when compared to diesel and ethanol fuel engine shown in Figure 4.8.

ISSN (Online) 2456-1290

International Journal of Engineering Research in Mechanical and Civil Engineering (IJERMCE)
Vol 3, Issue 2, February 2018

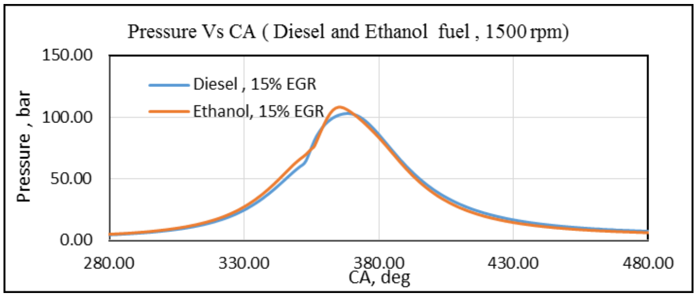

Figure 4.9 Pressure Vs CA Comparison of Diesel and Ethanol fuel,1500 rpm, 0.222 g/Cycle, 15% EGR

It can be shown that variation In-Cylinder Pressure with respect to CA and shown in Figure 4.9, In-cylinder Pressure with CA diagram shows that when increasing the EGR ratio 15% the variation of peak pressure is not drastically changed concerning EGR and compared to diesel and ethanol fuel shown in Figure 4.9.

5 Conclusion

Multi-cylinder Preheated turbocharged high compression ignition engine simulation and experimental results were used to predict the following conclusion. Diesel RK Simulation and experimental results are used to obtain the following conclusion is.

SFC, NOx, PM, and ID of three different EGR with different CFM are plotted with different EGR and investigated. SFC, NOx, PM, and ID of and rate of heat release are predicted and plotted.

The premixed combustion zone heat release rate with EGR is higher compared to 0% EGR. The Heat release rate curve shifted to two deg BTDC due to increasing the evaporation.

Intake Air temperature is increased from 200 to 450c by using the preheated turbocharged system, and this technology was supported to increase the in-cylinder temperature and initiate better combustion compare to 0% EGR mode.

In-cylinder Pressure does not drastically change for comparison of ethanol and diesel fuel with and without the EGR mode test due to the high latent evaporation of ethanol fuel.

1) SFC of 15 % EGR at all CFM is slightly higher with 0 % EGR for diesel and ethanol fuel engines.

2) NOx of 15% EGR mode at all load conditions drastically reduced compared to with 0% EGR mode for both diesel and ethanol mode operation. NOx emission was 78% lower than 0% EGR for ethanol and 68% lower than diesel mode.

3) PM of ethanol fuel engine is significantly lower than others shown in sections 3 and 4; hence ethanol was soot-free combustion compared to a diesel engine.

Ignition Delay (ID) of ethanol fuel engine is two to four degrees lower than 0% EGR mode at different CFM, as shown in section 3. Low ID was also one of the added advantages of other parameters for the selection of performance parameters. Based on the detailed analysis, the combustion was better and low emission for 15% EGR mode and selected for base fuel diesel and better combustion ethanol fuel for multi-cylinder preheated turbocharged High compression ignition engine.

Nomenclature

Up	-	Average Piston Speed
BDC	-	Bottom Dead Center
BMEP	-	Brake Mean Effective Pressure
BP	-	Brake Power
BSFC	-	Brake Specific Fuel Consumption
BTE	-	Brake Thermal Efficiency
CO2	-	Carbon Dioxide
CO	-	Carbon Monoxide
CN	-	Cetane Number
CR	-	Compression Ratio
CFR	-	Cooperative Fuel Research
CA	-	Crank Angle
CFM	-	Cycle Fuel Mass
DI	-	Direct Injection
EGR	-	Exhaust Gas Recirculation
FP	-	Friction Power
GHG	-	Green House Gas
HSU	-	Hartridge Smoke Unit
HC	-	Hydro Carbon
IMEP	-	Indicated Mean Effective Power
IP	-	Indicated Power
ITE	-	Indicated Thermal Efficiency
IDI	-	Indirect Injection
ICE	-	Internal Combustion Engine
ISO	-	International Standard Organisation
MTBE	-	Methyl Tetra Butyl Ether
NWR	-	Near Wall Flow
NOx	-	Nitrous Oxide
NDIR	-	Non-Dispersive Infrared Analyser
PM	-	Particulate Matter
PEG	-	Poly Ethylene Glycol
SFC	-	Specific Fuel Consumption
SOC	-	Start of Combustion
SOI	-	Start of Injection
SR	-	Swirl Ratio
Ut	-	Swirl Tangential Speed
TDC	-	Top Dead Center
TFC	-	Total Fuel Consumption

UHC - Unburned Hydro Carbon
VCR - Variable Compression Ratio

Acknowledgement

I give my very hearty thanks to my supervisor A.S. Krishnan, Dr G Sureshkannan, associate professor, Dr K Marimuthu, head of mechanical engineering department, Dr V Selladurai, principal, Coimbatore Institute of Technology, Coimbatore, for all encouragement during this research.

Reference

[1] A. Demirbas, "Progress and recent trends in biofuels," Prog. Energy Combust. Sci., vol. 33, no. 1, pp. 1–18, 2007.
[2] H. Chen, J. Wang, S. Shuai, and W. Chen, "Study of oxygenated biomass fuel blends on a diesel engine," Fuel, vol. 87, no. 15–16, pp. 3462–3468, 2008.
[3] S. Kimura, O. Aoki, Y. Kitahara, and E. Aiyoshizawa, "Ultra-Clean Combustion Technology Combining a Low-Temperature and Premixed Combustion Concept for Meeting Future Emission Standards," 2001.
[4] N. Raeie, S. Emami, and O. Karimi Sadaghiyani, "Effects of injection timing, before and after top dead centre on the propulsion and power in a diesel engine," Propuls. Power Res., vol. 3, no. 2, pp. 59–67, 2014.
[5] A. S. Kuleshov, "Model for predicting air-fuel mixing, combustion and emissions in DI diesel engines over the whole operating range," 2005.
[6] C. D. Rakopoulos, D. C. Rakopoulos, D. T. Hountalas, E. G. Giakoumis, and E. C. Andritsakis, "Performance and emissions of bus engine using blends of diesel fuel with bio-diesel of sunflower or cottonseed oils derived from Greek feedstock," Fuel, vol. 87, no. 2, pp. 147–157, 2008.
[7] J. Jonathan Chaplin and R. Bin Rimfiel Bin Janus, "Ethanol Fumigation of a Compression-Ignition Engine Using Advanced Injection of Diesel Fuel," Trans. ASAE, vol. 30, no. 3, pp. 0610–0614, 1987.
[8] C. C. D. Rakopoulos, G. N. G. Taklis, and E. E. I. Tzanos, "Analysis of combustion chamber insulation effects on the performance and exhaust emissions of a DI diesel engine using a multi-zone model," Heat Recover. Syst. CHP, vol. 15, no. 7, pp. 691–706, Oct. 1995.
[9] N. Saravanan, G. Nagarajan, G. Sanjay, C. Dhanasekaran, and K. M. Kalaiselvan, "Combustion analysis on a DI diesel engine with hydrogen in dual fuel mode," Fuel, vol. 87, no. 17–18, pp. 3591–3599, 2008.
[10] K. P. Kumar and K. Yuvaraj, "Analysis of Performance and Emission Parameters on Diesel Engine Using Various Blended Bio-Fuels," vol. 5, no. 6, pp. 1319–1324, 2016.
[11] A. S. Kuleshov, A. V Kozlov, and K. Mahkamov, "Self-Ignition delay Prediction in PCCI direct injection diesel engines using multi-zone spray combustion model and detailed chemistry," 2010.
[12] A. J. Smith, D. H. Tidmarsh, M. F. J. Brunt, and M. Wilcock, "The impact of the start of injection timing and EGR rate on the emissions performance of a modern high-speed DI diesel engine," Automot. Engines Powertrains - Autotech '97, vol. 97, no. 6, pp. 145–154, 1997.
[13] B. Rajesh Kumar and S. Saravanan, "Use of higher alcohol biofuels in diesel engines: A review," Renew. Sustain. Energy Rev., vol. 60, pp. 84–115, 2016.
[14] L. Xing-cai, Y. Jian-Guang, Z. Wu-gao, and H. Zhen, "Effect of cetane number improver on heat release rate and emissions of a high-speed diesel engine fueled with ethanol–diesel blend fuel," Fuel, vol. 83, no. 14, pp. 2013–2020, 2004.
[15] J. Liu, G. Li, and S. Liu, "Influence of Ethanol and Cetane Number (CN) Improver on the Ignition Delay of a Direct-Injection Diesel Engine," Energy & Fuels, vol. 25, no. 1, pp. 103–107, Jan. 2011.
[16] R. Munson, Y. Laoonual, S. Jugjai, M. Matsuki, and H. Kosaka, "Investigation of effects of ignition improvers on ignition delay time of ethanol combustion with rapid compression and expansion machine," SAE Tech. Pap., no. February 2012.
[17] N. Ghassembaglou and L. Torkaman, "Efficient design of exhaust gas cooler in cold EGR equipped diesel engine," Alexandria Eng. J., vol. 55, no. 2, pp. 769–778, 2016.
[18] G. S. Hebbar and A. K. Bhat, "Control of NOx from a DI diesel engine with hot EGR and ethanol fumigation: An experimental investigation," Int. J. Automot. Technol., vol. 14, no. 3, pp. 333–341, 2013.
[19] A. S. Kuleshov, "Multi-Zone DI Diesel Spray Combustion Model for Thermodynamic Simulation of Engine with PCCI and High EGR Level," 2009.
[20] M. F. Al-Dawody and S. K. Bhatti, "Theoretical modelling of combustion characteristics and performance parameters of biodiesel in DI diesel engine with variable compression ratio," vol. 4, no. 2, pp. 231–242, 2013.
[21] A. Kuleshov, K. Mahkamov, A. Kozlov, and Y. Fadeev, "Simulation of Dual-Fuel Diesel Combustion With Multi-Zone Fuel Spray Combustion Model," Vol. 2 Instrumentation, Control. Hybrids; Numer. Simulation; Engine Des. Mech. Dev. Keynote Pap., p. V002T06A020, 2014.
[22] S. A. Siddique, K. Vijaya, and K. Reddy, "Experimental Validation and Combustion Chamber Geometry Optimization of Diesel Engine By Using Diesel –

Rk," Int. J. Mech. Eng. Technol., vol. 6, no. 2, pp. 976–6340, 2015.
[23] M. Huo, S. Lin, H. Liu, and C. F. F. Lee, "Study on the spray and combustion characteristics of water-emulsified diesel," Fuel, vol. 123, 2014.
[24] B. Jayashankara and V. Ganesan, "Effect of fuel injection timing and intake pressure on the performance of a di diesel engine - A parametric study using CFD," Energy Convers. Manag., vol. 51, no. 10, pp., 1835–1848, 2010.
[25] E. Porpatham, A. Ramesh, and B. Nagalingam, "Effect of swirl on the performance and combustion of a biogas fuelled spark ignition engine," Energy Convers. Manag., vol. 76, pp. 463–471, 2013.
[26] A. Schaefer and H. O. Hardenberg, "Ignition Improvers for Ethanol Fuels," SAE Technical Paper, vol. 810249. p. 9, 1981.
[27] H. K. Imdadul et al., "Influences of ignition improver additive on a ternary (diesel-biodiesel-higher alcohol) blends thermal stability and diesel engine performance," Energy Convers. Manag., vol. 123, pp. 252–264, 2016.